NUREG/CR-6784

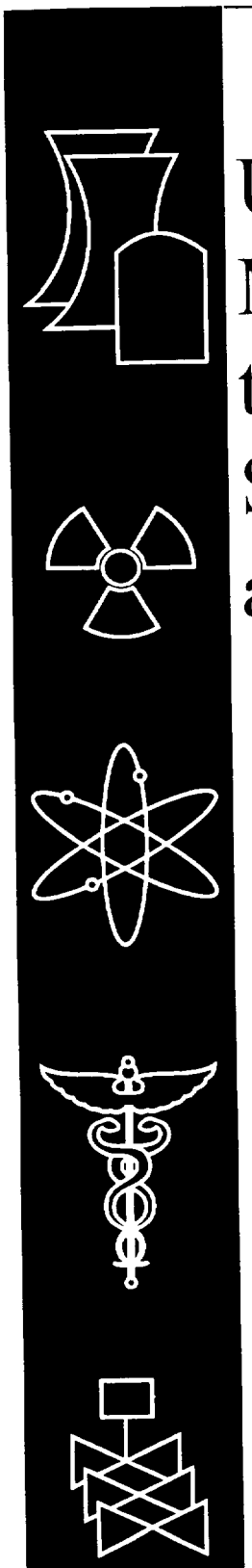

Use of Computerized Microtomography to Examine the Relationships of Sorption Sites in Alluvial Soils to Iron and Pore Space Distributions

Sandia National Laboratories

U.S. Nuclear Regulatory Commission
Office of Nuclear Regulatory Research
Washington, DC 20555-0001

AVAILABILITY OF REFERENCE MATERIALS IN NRC PUBLICATIONS

NRC Reference Material

As of November 1999, you may electronically access NUREG-series publications and other NRC records at NRC's Public Electronic Reading Room at www.nrc.gov/NRC/ADAMS/index.html. Publicly released records include, to name a few, NUREG-series publications; *Federal Register* notices; applicant, licensee, and vendor documents and correspondence; NRC correspondence and internal memoranda; bulletins and information notices; inspection and investigative reports; licensee event reports; and Commission papers and their attachments.

NRC publications in the NUREG series, NRC regulations, and *Title 10, Energy*, in the Code of *Federal Regulations* may also be purchased from one of these two sources.

1. The Superintendent of Documents
   U.S. Government Printing Office
   Mail Stop SSOP
   Washington, DC 20402–0001
   Internet: bookstore.gpo.gov
   Telephone: 202-512-1800
   Fax: 202-512-2250
2. The National Technical Information Service
   Springfield, VA 22161–0002
   www.ntis.gov
   1–800–553–6847 or, locally, 703–605–6000

A single copy of each NRC draft report for comment is available free, to the extent of supply, upon written request as follows:

Address: Office of the Chief Information Officer,
Reproduction and Distribution
Services Section
U.S. Nuclear Regulatory Commission
Washington, DC 20555-0001
E-mail: DISTRIBUTION@nrc.gov
Facsimile: 301–415–2289

Some publications in the NUREG series that are posted at NRC's Web site address www.nrc.gov/NRC/NUREGS/indexnum.html are updated periodically and may differ from the last printed version. Although references to material found on a Web site bear the date the material was accessed, the material available on the date cited may subsequently be removed from the site.

Non-NRC Reference Material

Documents available from public and special technical libraries include all open literature items, such as books, journal articles, and transactions, *Federal Register* notices, Federal and State legislation, and congressional reports. Such documents as theses, dissertations, foreign reports and translations, and non-NRC conference proceedings may be purchased from their sponsoring organization.

Copies of industry codes and standards used in a substantive manner in the NRC regulatory process are maintained at—

The NRC Technical Library
Two White Flint North
11545 Rockville Pike
Rockville, MD 20852–2738

These standards are available in the library for reference use by the public. Codes and standards are usually copyrighted and may be purchased from the originating organization or, if they are American National Standards, from—

American National Standards Institute
11 West 42nd Street
New York, NY 10036–8002
www.ansi.org
212–642–4900

Legally binding regulatory requirements are stated only in laws; NRC regulations; licenses, including technical specifications; or orders, not in NUREG-series publications. The views expressed in contractor-prepared publications in this series are not necessarily those of the NRC.

The NUREG series comprises (1) technical and administrative reports and books prepared by the staff (NUREG–XXXX) or agency contractors (NUREG/CR–XXXX), (2) proceedings of conferences (NUREG/CP–XXXX), (3) reports resulting from international agreements (NUREG/IA–XXXX), (4) brochures (NUREG/BR–XXXX), and (5) compilations of legal decisions and orders of the Commission and Atomic and Safety Licensing Boards and of Directors' decisions under Section 2.206 of NRC's regulations (NUREG–0750).

NUREG/CR-6784

Use of Computerized Microtomography to Examine the Relationships of Sorption Sites in Alluvial Soils to Iron and Pore Space Distributions

Manuscript Completed: June 2002
Date Published: July 2002

Prepared by:
A.A. McLain[1], S.J. Altman[1], M.L.Rivers[2], and R.T. Cygan[3]

[1]Geohydrology Department, Sandia National Laboratories, Albuquerque, NM 87185-0735
[2]CARS, University of Chicago, 5640 S. Ellis Ave., Chicago, IL 60637
[3]Geochemistry Department, Sandia National Laboratories, Albuquerque, NM 87185-0750

Sandia National Laboratories
Albuquerque, NM 87185-0750

E. O'Donnell, NRC Project Manager

Prepared for:
Division of Systems Analysis and Regulatory Effectiveness
Office of Nuclear Regulatory Research
U.S. Nuclear Regulatory Commission
Washington, DC 20555-0001
NRC Job Code W6811

Abstract

This report presents results from computerized microtomographic (CMT) imaging of soils from Naturita, Colorado, a Uranium Mill Tailings Remedial Action (UMTRA) site. The objective is to better understand the mineralogical and morphological controls of the sorption of uranium in the sediment. The samples were prepared and imaged with three goals in mind: 1) to visualize iron-rich mineral distribution in fine-grained materials (<355 μm grain size) and aggregate grains, 2) to visualize pore space in the aggregates, and 3) to visualize cesium sorption sites as a proxy for uranium. Two sets of images were obtained with voxel sizes of 6.7 μm and 3.3 μm on a side, respectively. Bright rims with a thickness of 4 to 15 μm were observed on fine-grained materials and aggregate grains. Porous, iron-rich interstitial material was also observed within the aggregates. It is speculated that these interstitial materials are clay minerals closely associated with some iron oxyhydroxide phases or iron oxyhydroxides that are porous at the sub-micron scale. However, to verify this identification, the CMT data needs to be post-processed using calibration materials to minimize noise and error. A subtraction technique using images obtained just above and below the X-ray absorption edges of iodine and cesium successfully illustrates the pore space distribution in the KI-saturated samples and sorption sites in CsCl-treated samples. The cesium sorption sites appear to be associated with accessible pore space observed in the untreated and KI-saturated samples. The cesium sorption sites are also associated with iron-rich areas both as exterior coatings and in the interstitial areas of the aggregate grains.

Contents

Figures

Acknowledgments

The authors would like to acknowledge the helpful discussions with James Davis, Edward O'Donnell, and Henry Westrich during the course of the research. Vincent Tidwell provided a valuable review of the original manuscript that greatly benefitted the final paper. We would also like to thank Steven Thoma for providing the BET surface area data and Howard Anderson for assisting in collection of the SEM images. This work was supported by the U.S. Nuclear Regulatory Commission, Office of Nuclear Regulatory Research. We are very grateful for the advice and support provided by our NRC program manager Edward O'Donnell during the funding period. Sandia National Laboratories is a multi-program laboratory operated by the Sandia Corporation, a Lockheed Martin Company, for the United States Department of Energy under Contract DE-AC04-94AL85000.

1. Introduction

1.1 Background

Synchrotron computerized microtomography (CMT) is a recent method that offers the ability to characterize the sorptive properties of minerals associated with alluvial soils. In particular, a relationship between metal sorption sites, iron-bearing minerals, and pore-space distribution can be derived to help evaluate the mechanisms of sorption processes. Sorption onto clays and iron oxyhydroxide phases is an important process in the retardation of certain solutes in the subsurface environment (Jenne, 1998). Understanding the relationship between the physical properties of the subsurface materials with the sorption of metals onto the media enhances the ability to predict the transport and ultimate fate of hazardous chemicals and radioactive species in the environment.

This study is part of a larger cooperative project involving the U. S. Geological Survey (USGS), the U. S. Nuclear Regulatory Commission (NRC), and Sandia National Laboratories (SNL) being performed at the Naturita Uranium Mill Tailings Remedial Action Project (UMTRA) site in Colorado (Figure 1). The overall study integrates results of fundamental theory and experiments with field measurements to better understand the complex nature of sorption of radionuclides onto mineral surfaces. Other components of the research project include soil characterization (Jové Colón et al., 2002), column experiments (Curtis et al., 2001; Kohler et al., 2001), uncertainty analysis (Criscenti et al., 2002), and molecular modeling (Teter and Cygan, 2002).

The goal of the soil characterization task is to better understand the mineralogical and morphological controls of the sorption of uranium in the soil and sediment. These controls include the distribution of sorption sites among the soil minerals, and the pore space distribution, which allows access to the sorption sites for infiltrating fluids. Scanning Electron Microscopy-Energy Dispersive Spectrometry (SEM-EDS), Secondary Ion Mass Spectrometry (SIMS), High Resolution Transmission Electron Microscopy (HRTEM), and Micro-Synchrotron X-Ray Fluorescence (M-SXRF) have been used to characterize clays and iron oxyhydroxide minerals in the soils in uncontaminated and contaminated alluvium from the Naturita site (Jové Colón et al., 2002). The M-SXRF investigation, for example, demonstrated a strong correlation between uranium sorption and the iron-rich regions of the mineral coatings.

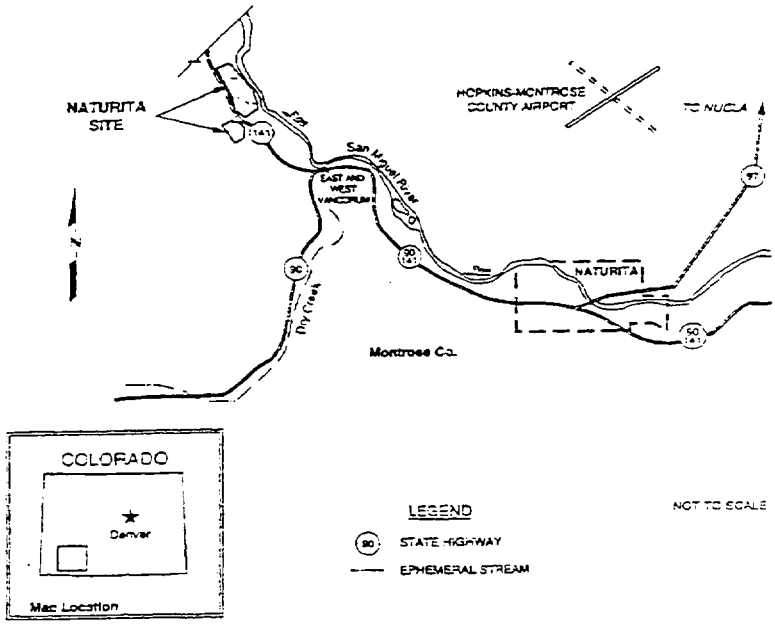

Figure 1. Location of Naturita UMTRA site in southwestern Colorado (from Davis et al., 1999).

Soil samples were collected from the alluvial plain of the San Miguel River several hundred yards upstream of the site of the former uranium processing mill. The uncontaminated composite sample is comprised of poorly sorted sediment and includes fractions ranging from sub-micron fine particles to large cobbles with diameters in excess of 10 cm. Sieving and processing of the alluvial materials by the USGS provided two sets of representative samples for the analysis and characterization of the mineral coatings (Figure 2): fine-grained materials and cemented aggregate grains. The fine-grained materials consist mainly of sub-rounded to sub-angular grains of quartz and potassium feldspar plus a clay-sized fraction (Figure 2a). The aggregate samples are comprised mainly of quartz and potassium feldspar sub-rounded to rounded grains that are bridged by platy clay coatings (Figure 2b). The grains also are coated by platy to lathlike clay minerals and iron oxyhydroxide phases.

The coatings and interstitial materials have been difficult to characterize by traditional mineralogical methods, such as X-ray diffraction, due to their fragile nature and occurrence as thin coatings (approximately 5 to 20 microns). The mineral coatings comprise less than 5% of the total material and contribute little to the intensity of the X-ray diffraction patterns obtained for each of the two soil samples. Attempts to mechanically and chemically process the soil samples, to enhance the proportion of coating phases relative to the substrate minerals, proved unsuccessful.

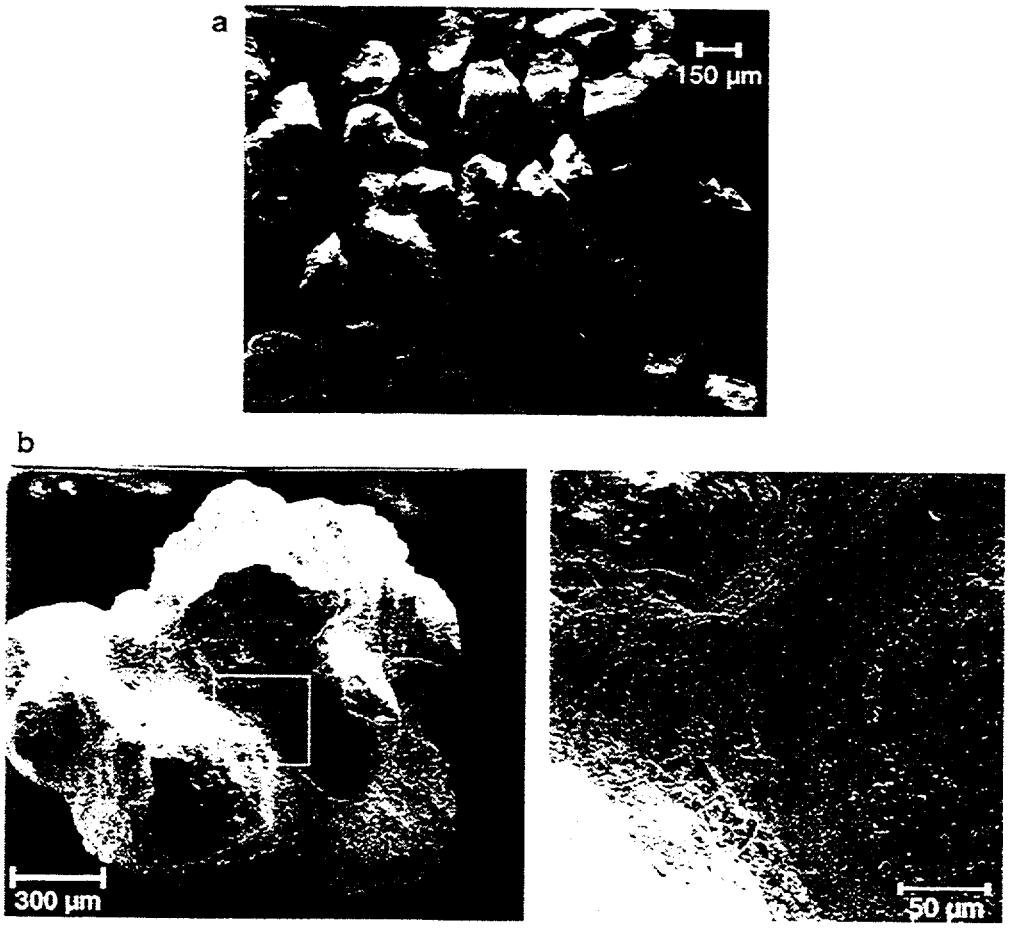

Figure 2. SEM images of (a) fine-grained materials and (b) cemented aggregate grains. Clay minerals can be seen to bridge and coat the grains in the aggregates.

This study explores the use of computerized microtomography (CMT) as a nondestructive, high-resolution method to enhance the characterization of soils in support of the general effort to fully describe and evaluate metal sorption in soils at Naturita and other uranium contaminated sites. Past efforts to characterize these kinds of soil materials have utilized destructive methods such as chemical leaching or thin-sectioning samples, or were limited to only imaging and analyzing the exterior surfaces of the sample (Jové Colón et al., 2002). With computerized microtomography, the interior and exterior of aggregate samples can be imaged intact. Because of the nondestructive nature of CMT, the method can be used to examine the complex relationship among coating mineralogy, sorption sites, and pore space. Brunauer, Emmitt, and Teller (BET) gas sorption analysis of the two samples was also performed to provide a conventional bulk surface area measurement for comparison with the CMT results.

Computerized microtomography is utilized in this study to achieve three goals:

1. Visualize mineralogical differences and iron-rich coatings in aggregates and fine-grained material,

2. Visualize accessible pore space in aggregates, and

3. Visualize cesium (Cs^{+}) sorption sites in aggregated grains, with cesium acting as a proxy for sorbed uranium species such as the uranyl (UO_2^{2+}).

1.2 Application of Computerized Microtomography

Computerized microtomography is a nondestructive analytical technique that generates high-resolution (<10 μm) three-dimensional images of the absorption of X-rays by a material. It has been successfully used in a number of geological applications, such as characterization of porosity in sandstones (Spanne et al., 1994; Schwartz et al., 1994; Coker and Torquato, 1996), characterization of metamorphic textures (Denison et al., 1997), and characterization of water content in soils (Macedo et al., 1999).

The first step in CMT analysis is the collection of X-ray absorption data. A synchrotron-derived, well-collimated, monochromatic X-ray beam passes through a sample mounted on a rotating stage. X-rays transmitted through the sample are converted to visible light with a phosphor plate and recorded by a charged-couple device (CCD) camera. The sample is rotated and imaged in evenly spaced increments between 0 and 180 degrees. A three-dimensional image is then reconstructed from the set of two-dimensional projections by Fourier transformations. Detailed descriptions of the tomographic reconstruction process and limitations of CMT are available in Herman (1980) and Flannery et al. (1987). In the final reconstructed image, the object of interest is represented by an array of volume elements (voxels) in three dimensions. The data value at each voxel is the linear x-ray absorption coefficient, μ. Two-dimensional arrays of picture elements (pixels) can be easily extracted from the three-dimensional image (Figure 3). Theoretical X-ray transmission through a sample can be calculated using Beer's Law:

$$\frac{I}{I_o} = \exp(-\mu x) \tag{1}$$

where I_o is the source X-ray intensity, I is the transmitted X-ray intensity, x is the distance the X-ray travels through the sample (or the sample thickness [L]), and μ is the linear absorption coefficient [1/L]. Tabular data is available for the linear absorption coefficient as a function of X-ray energy for each element (e.g., McMaster et al., 1969).

If a material consists of multiple elements, like most geologic samples, then the transmitted X-ray intensity can be calculated as follows:

$$\frac{I}{I_o} = \exp\left(-\left[f_1\mu_{m1} + f_2\mu_{m2} + f_3\mu_{m3} + \ldots\right]\rho x\right) \tag{2}$$

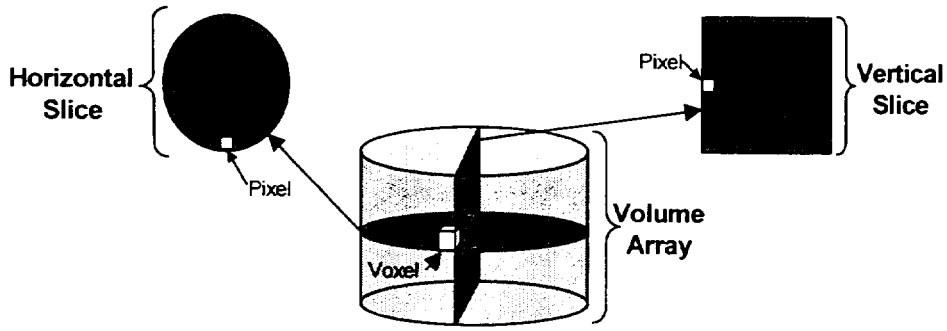

Figure 3. Schematic representation of three-dimensional volume data array generated by the CMT reconstruction process. Figures 5 – 7 present two-dimensional vertical or horizontal slices that have been extracted from volume arrays.

where f_1, f_2, f_3 are the mass fractions of elements 1, 2, 3, etc., ρ is the density of the composite material [M/L^3], and x is the material thickness [L]. The mass absorption coefficient, μ_m [L^2/M], of each element is defined as the linear absorption coefficient of the element divided by the density of the element, (e.g., m_1/r_1).

By combining Equations (1) and (2), the theoretical linear absorption coefficient of a mineral can be calculated if its elemental composition is known:

$$\mu = \left[f_1 \mu_{m1} + f_2 \mu_{m2} + f_3 \mu_{m3} + \ldots \right] \rho \tag{3}$$

A useful property of X-ray absorption is the "absorption edge," which is the energy required to remove an electron from an inner shell of the atom. The absorption edge results in an abrupt change in X-ray absorption at a characteristic X-ray energy for individual elements. At an energy just below an absorption edge an element is much less absorbing to X-rays than at energies immediately above the absorption edge. Figure 4 depicts the change in the linear absorption coefficient (m) with increasing X-ray energy for three elements which are of interest in this study: cesium, iodine, and iron. There is an abrupt increase in m at energies of 33.2 keV for iodine and 36.1 keV for cesium. Note that iron does not have an absorption edge in the energy range shown in Figure 4. We take advantage of this absorption edge in CMT by using an image subtraction technique explained in Section 2.3.2. The subtraction method can be used to enhance areas in a sample containing only a particular element, in this case iodine or cesium.

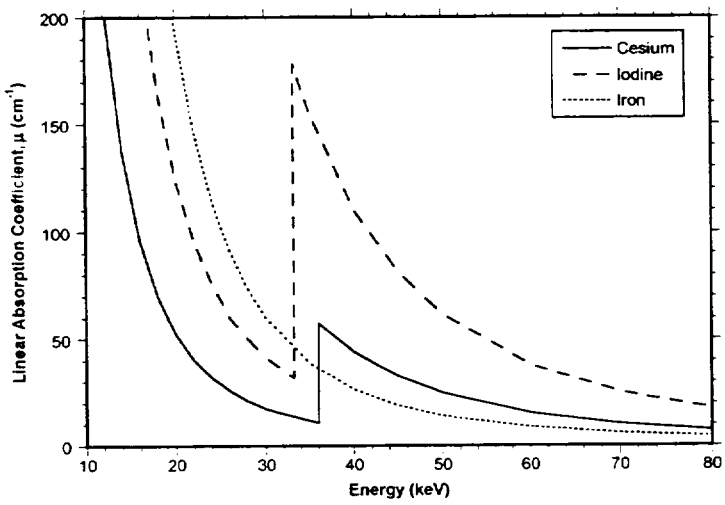

Figure 4. Variation in linear absorption coefficient (μ) with X-ray energy for cesium, iodine, and iron. Note the sharp increases at the absorption edges of 33.2 keV for iodine and 36.1 keV for cesium. Iron does not have the same sharp increase in this energy range. Data are from McMaster et al., 1969.

2. Methods

2.1 Sample Preparation

Three subgroups of samples from the two sediment types of uncontaminated Naturita soils were prepared for the CMT imaging (Table 1): 1) untreated aggregate grains and fine-grained separates for imaging the iron-rich coatings, 2) aggregate grains saturated with KI solution for pore-space visualization, and 3) aggregate grains treated with CsCl solution and rinsed to visualize sorption sites. Aggregate grains ranging in diameter from approximately 1 to 2 mm were hand-picked from the composite sample. Fine-grained materials were size separated using a No. 45 mesh size sieve to a grain size of less than 355 microns.

Table 1. Sample summary and X-ray energies for CMT analysis.

Treatment	Tracer Concentration	Sample Material	Energy at which images were obtained (keV)	Voxel Size on a Side (μm)
Untreated	N/A	Aggregate Fine-grained	25.00	6.7
Untreated	N/A	Aggregate	20.00	3.3
KI Saturated	2.4 M (300 g/L) I	Aggregate	33.03 and 32.93	6.7
CsCl Treated	3.2 M (400 g/L) Cs	Aggregate	36.05 and 35.95	6.7

Two methods were used to mount the samples so they could be imaged using CMT. All three sets of samples were packed in 2.6-mm inner diameter glass pipette tubes with quartz wool at either end to seal the tubes. In addition, the individual untreated aggregate grains were mounted on the end of toothpicks. This second mounting method allowed for higher resolution of the CMT because of the smaller sample dimensions (see Section 2.2).

Both the KI-saturated samples and the CsCl-treated samples were vacuum saturated overnight in their respective solutions (Table 1). The capillary tubes were sealed on either end with plumber's epoxy. Additional quartz wool was packed around aggregates in the KI-saturated samples to reduce the volume of solution around the aggregates and to help reduce X-ray absorption around the sample.

Shortly before imaging, the CsCl-treated samples were rinsed with deionized water. The glass tubes were fitted with a reservoir containing the deionized water on one end and a hand-held vacuum pump on the other. At least 10 column volumes of rinse water were passed through the sample. The effluent from the rinse process was verified to be free of Cl by testing for silver chloride precipitation with silver nitrate solution. Given this verification and the fact that the solubility of CsCl at 25°C is greater than 11 M (Lide, 1991), the occurrence of CsCl precipitation on or in the aggregates is thought to be unlikely. The cesium imaged in these samples is assumed to represent the strongly bonded sorption sites present in the aggregates (Krumhausl et al., 2001).

In addition to imaging the samples described in Table 1, capillary tubes filled with known concentrations of CsCl (20, 50, 100, and 400 gCs/L) and aluminum, titanium, and cobalt wires were also imaged. These data were collected to evaluate the error and background signal associated with the CMT setup.

2.2 Computerized Microtomography Data Collection

All samples were imaged and reconstructed using the CMT facility at beamline BM-13-D, GeoSoilEnvironCARS, at the Advanced Photon Source (APS) of Argonne National Laboratory (Rivers et al., 1999). The samples were rotated at 0.25 degree increments between 0 and 180 degrees. The energies and resultant voxel sizes of the imaging are listed in Table 1. Image sets of the KI-saturated samples were obtained above and below the absorption edges for iodine (33.03 keV and 32.93 keV). Image sets of the CsCl-treated samples were obtained above and below the absorption edges for cesium (36.05 keV and 35.95 keV). Both sets of CMT images were collected at two different energy levels

so that the subtraction method to enhance iodine and cesium visualization could be employed (see Section 2.3.2). It took approximately 45 minutes to obtain one three-dimensional image.

On August 8-10, 2001 the lower-resolution images with a vertical dimension of 4.4 mm were obtained. These images included seven images of the untreated aggregates, each containing two to three aggregated grains; one image of the fine-grained material; three sets images of the KI-saturated sample; five sets of images of the CsCl-treated sample; and one image of the materials to perform the error analysis. Nine sets of higher-resolution images of aggregate grains were collected on April 6-8, 2002. These images were 2.3 mm in height. Three of these aggregates were subsequently treated with CsCl, as described in Section 2.1, and imaged above and below the absorption edge of cesium. The high-resolution images were obtained by using a higher magnification objective lens and adjusting the tube length between the lens and the CCD. This was possible because of the smaller sample dimensions of the individual grains as compared to the samples contained in the capillary tubes.

2.3 Computerized Microtomography Data Analysis

Three different methods were used to analyze the CMT data. First, a qualitative analysis was made to determine the iron content in the samples. Second, a subtraction method was used to enhance the visualization of iodine and cesium. Lastly, CMT data from the capillary tubes filled with CsCl and metallic wires were used to evaluate the error and background signal of the CMT technique.

2.3.1 Determination of Iron Content of Samples

A qualitative evaluation of the iron content and spatial distribution was made of the fine-grained and aggregate samples. The differences in linear absorption coefficients between high atomic number elements and low atomic number elements were used to help distinguish the iron-rich areas in the images. Quartz and feldspars have low linear absorption coefficients (estimated using Equation (2) to be less than 6.6 cm^{-1} at an X-ray energy of 20 keV); clay minerals have intermediate values (approximately 10 cm^{-1} at an X-ray energy of 20 keV; values will vary with clay composition); and iron oxyhydroxide phases have relatively high values (estimated at 60-68 cm^{-1} at an energy of 20 keV). The higher the linear absorption coefficient, the brighter the area in an image. Therefore, iron oxyhydroxide coatings are expected to stand out as much brighter areas in the CMT images.

2.3.2 CMT Subtraction Method for Enhanced Visualization of Iodine and Cesium

As mentioned earlier, the project took advantage of the fact that the absorption edge of iodine (33.2 keV) and cesium (36.1 keV) fall within a reasonable energy range to develop a subtraction method technique to enhance the visualization of iodine and cesium. Two sets of images of the KI-saturated and CsCl-treated samples were collected; one at an X-ray energy slightly above the absorption edge, and one slightly below (Table 1). The sample is imaged in the identical position for both energies. By subtracting the voxel values in each position of the image taken above the absorption edge from the image taken below the edge, a new data array is generated, referred to as the difference image. If regions in the sample contain no iodine or cesium, the voxel values above and below the edge will be essentially the same, and therefore have zero intensity in the difference image. In contrast, if a sample region contains iodine or cesium, the voxel values in the difference image should be greater than zero and will appear as bright areas in the image. The difference image therefore enhances the visibility of the iodine occupying pore space in the sample or the cesium preferentially sorbed to the surface of the minerals.

2.3.3 Error and Noise Analysis

As mentioned above, images were collected of 20, 50, 100, and 400 gCs/L solutions and aluminum, titanium, and cobalt wires. The measured linear coefficient data were compared to the theoretical values as calculated using Equation (3).

The average measured linear absorption coefficient was determined by examining 100 horizontal slices of the tomographic image for each material. For each slice, a region of interest (ROI) was defined that contained a portion of the sample with the least amount of interference from the surrounding materials, such as the glass tubes. Each slice was defined by approximately 900 voxels. The average and standard deviation of the voxel values were calculated for each slice. Means of the averages and standard deviations of the 100 slices were then calculated.

2.4 Surface Area Determination

BET surface area measurements were made of the fine-grained materials and the hand-picked aggregate grains. Surface areas were determined using a Quantachrome Autosorb with nitrogen as the adsorbant. Samples were outgassed under vacuum for 12 hours at 120°C. Qualitative determination of microporosity was made via inspection of isotherms over the relative pressure range of 10^{-5} to 10^{-2} and quantitative evaluation was made using Deboer analysis of t-plots. Pore size distribution and total pore volume were calculated from the desorption branch of the isotherm using the BJH (Barett-Joyner-Halenda) model (Barrett et al.,1951).

3. Results and Discussion

3.1 Naturita Soil CMT Images

The results of the imaging of the untreated, KI-saturated, and CsCl-treated samples are presented in the form of two-dimensional gray scale images. Note that dark pixels represent areas with high X-ray transmission, or low-absorption by the material. Bright pixels are areas with low X-ray transmission, or high-absorption by the material.

3.1.1 Iron-Bearing Materials

Highly absorbing material, assumed to contain iron, is present in both the fine-grained materials and the aggregate soils (Figure 5). There are some grains in the fine-grained fractions of the sample that seem to be dominated by iron (white arrow in Figure 5a). The intermediate colored grains are assumed to be quartz or potassium feldspar. In addition, some grains appear to be coated by an iron-bearing material as can be seen by the bright rims around the grains (black arrow in Figure 5a).

Images of the aggregates clearly show that the interstitial material between the grains is iron-bearing (Figure 5b). The linear absorption coefficient measurements in these bright areas range from approximately 15 to 25 cm^{-1}, indicating that these materials are most likely clay minerals closely associated with some iron oxyhydroxide phases or iron oxyhydroxides that are porous at the sub-micron scale. However, to verify this identification, it would necessary to perform some post-processing to these data, as discussed in Section 3.2. Discontinuous bright rims are also seen around the aggregates (white arrow in Figure 5b). These coatings are estimated to have a thickness of 3.3 to 14.3 μm.

It is also interesting to note the dark areas in the bright interstitial materials. These dark areas are most likely micron-scale pore space, indicating that these interstitial materials are quite porous. In one case, a grain is clearly separated from the remainder of the aggregate, leaving an unobstructed flow path (oval in Figure 5b). Intergranular areas devoid of cement material have also been observed. These areas provide obvious pathways for fluid infiltration into the aggregated grains.

Note that some of the bright rims around the grains and aggregates might be artifacts of the imaging process due to refraction of the X-ray beam through the edges of the grains. These artifacts were minimized in the higher-resolution images (Figure 5b) by decreasing the distance between the sample and the phosphor plate.

3.1.2 Pore Space

Iodine saturation was used to enhance the pore space of the samples and visualize areas accessible to fluid (Section 2.3.2). In the CMT image taken above the iodine absorption edge (Figure 6a), iodine and iron-bearing materials can be observed as bright areas. In addition, the quartz or potassium feldspar grains (intermediate gray) and air bubbles (darker gray) in the sample can be seen. The bright areas in the image taken below the iodine absorption edge (Figure 6b) only show the iron-bearing materials, as the iodine is not as highly absorbed at this energy. Finally, the bright areas in the difference image represent only iodine. Thus, the fluid-accessible pore space within the aggregate grains is shown in the difference image (Figure 6c).

The observation of pore space in the interstitial material of the aggregates in Figure 5b is consistent with what is observed in the KI-saturated samples (Figure 6). That is, the accessible pore space is located where there is iron-bearing interstitial material (see bottom grain in Figure 6). The iodine did not penetrate an aggregate that did not have much iron-bearing interstitial material (top grain in Figure 6). This observation suggests a correlation between the mineralogy of this material and accessible pore space. Ehrenberg (1993) and Aagard et al. (2000) have made similar observations in cemented sandstones, where precipitation of clay minerals actually preserves accessible porosity in the formation.

3.1.3 Cesium Sorption Sites

The signal subtraction method (Section 2.3.2) was also used to identify cesium sorption sites. Cesium is used as a proxy for examining uranyl sorption onto the Naturita materials. In this case, the sample was first saturated with CsCl and

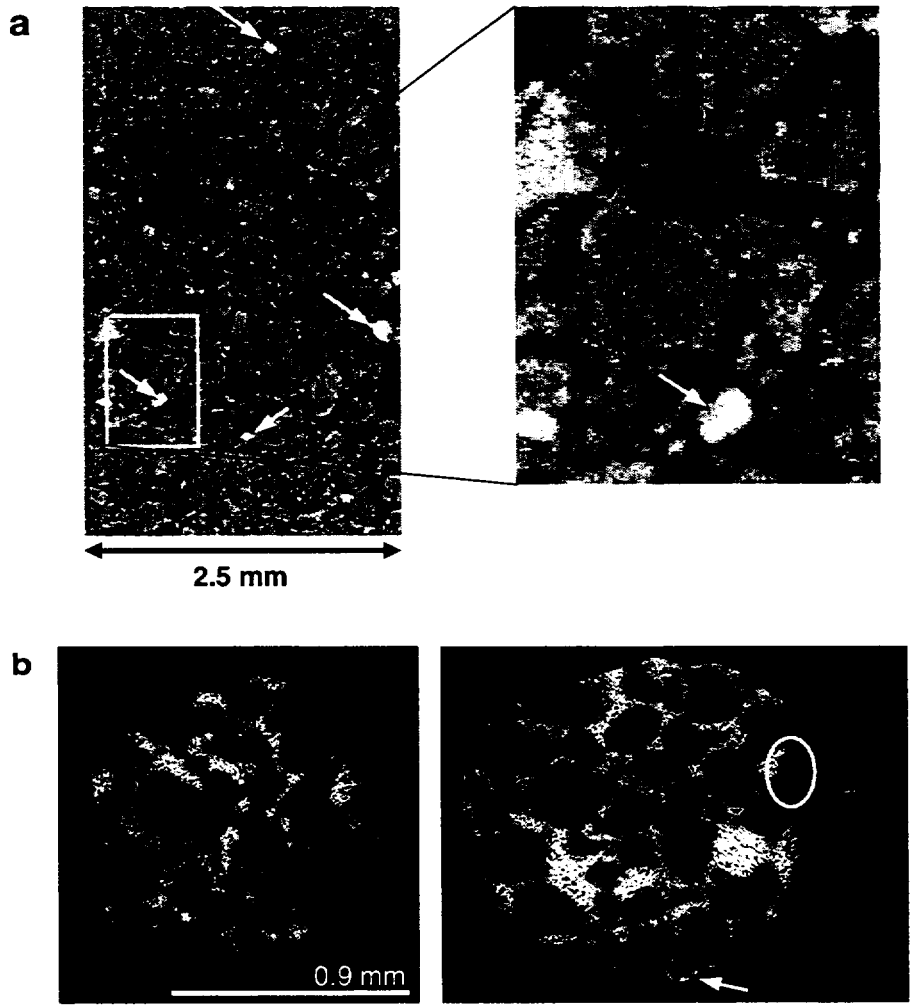

Figure 5. Vertical slice taken from CMT images of untreated fine-grained (a) and aggregate (b) samples. White arrows in (a) show highly X-ray absorbing grains. Dark arrows show highly absorbing coatings around the grains. The interstitial material between the grains of the aggregates is clearly highly absorbing to X-rays and also porous. Iron-bearing coatings also occur around the aggregates (white arrow in (b)). In one case, a high-porosity pathway occurs at a grain broken off of the aggregate (oval in (b)). Voxel sizes of images are 6.7 and 3.3 μm on a side for (a) and (b), respectively. Energies at which the images were obtained were 25.00 keV for (a) and 20.00 keV for (b).

then rinsed with deionized water. While there is a possibility that cesium has precipitated in the samples, this is unlikely, as rinsed with deionized water. While there is a possibility that cesium has precipitated in the samples, this is unlikely, as a small concentration of CsCl and the effluent from the rinse was used to ensure that the chloride had been removed (see Section 2.1).

Cesium sorption sites are clearly observed in some (Figure 7), but not all, aggregate samples. Cesium is seen both in the interior of an aggregate and on exterior coatings (Figure 7b). The location of the cesium sorption clearly can be correlated with accessible pore space (e.g., oval on Figure 7). Areas of cesium sorption are also associated with iron-bearing minerals (compare light areas in Figure 7a to those in 7b).

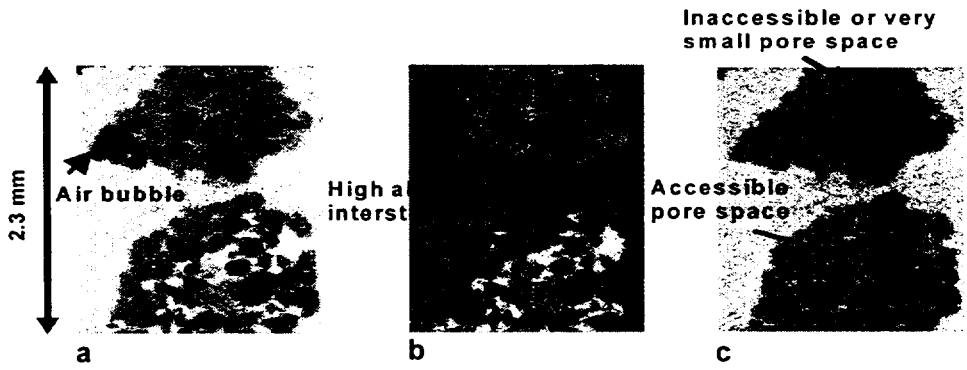

Figure 6. Vertical slices taken from the same position in three CMT images of an KI-saturated aggregate: (a) imaged above the iodine absorption edge (33.03 keV), (b) imaged below the absorption edge (32.93 keV), (c) difference image (a-b) which shows areas containing only iodine. The aggregate grains are easily discerned and are surrounded by the iodine solution. Note that more of the iodine penetrates into the interior of the aggregate with the high X-ray absorbance interstitial material. Voxel size of images is 6.7 μm on a side.

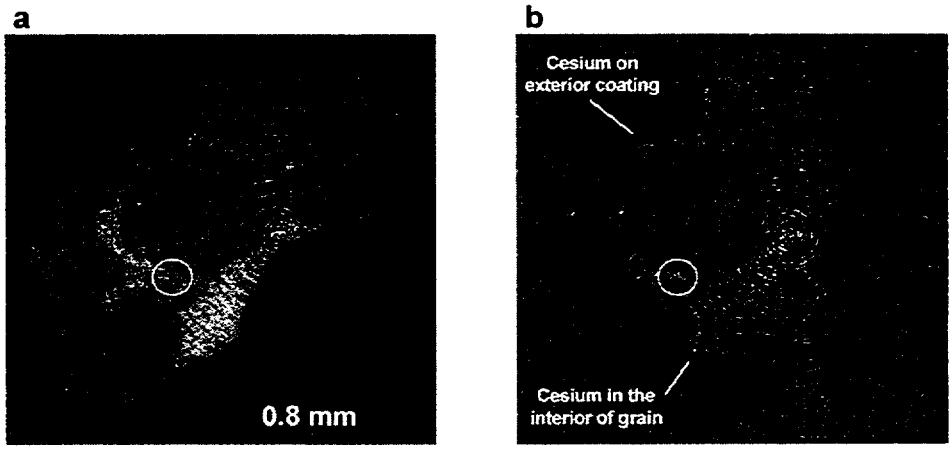

Figure 7. Image of an aggregate showing cesium sorption sites. (a) is taken below the cesium X-ray absorption edge (35.95 keV) showing areas of higher iron content (brighter areas). (b) is the difference image showing cesium sorption sites as the brighter areas. The cesium sorption sites appear to be associated with accessible pore space and iron-bearing minerals. Voxel size of images is 3.3 μm on a side.

3.2 CMT Error and Noise Analysis

The noise in the CMT imaging technique was evaluated by examining the mean and standard deviation of measured linear coefficients in materials of known and consistent values (see Sections 2.1 and 2.3.3). There is little variation in the mean linear coefficient over 100 slices taken through two wires (Figure 8a). This observation indicates that the X-ray beam energy was consistent over the vertical area through which it passed for the wires. Some spread in the measured linear coefficients was observed. The range over plus or minus two standard deviations, or 95% of the values, for these 100 slices is 1.8 – 3.3 cm^{-1}. This translates to a mean spread of 9.5% and 25% from the mean for cobalt and

titanium, respectively. A reduction in the background noise in future efforts with post-processing software is expected to normalize the data to the known theoretical values.

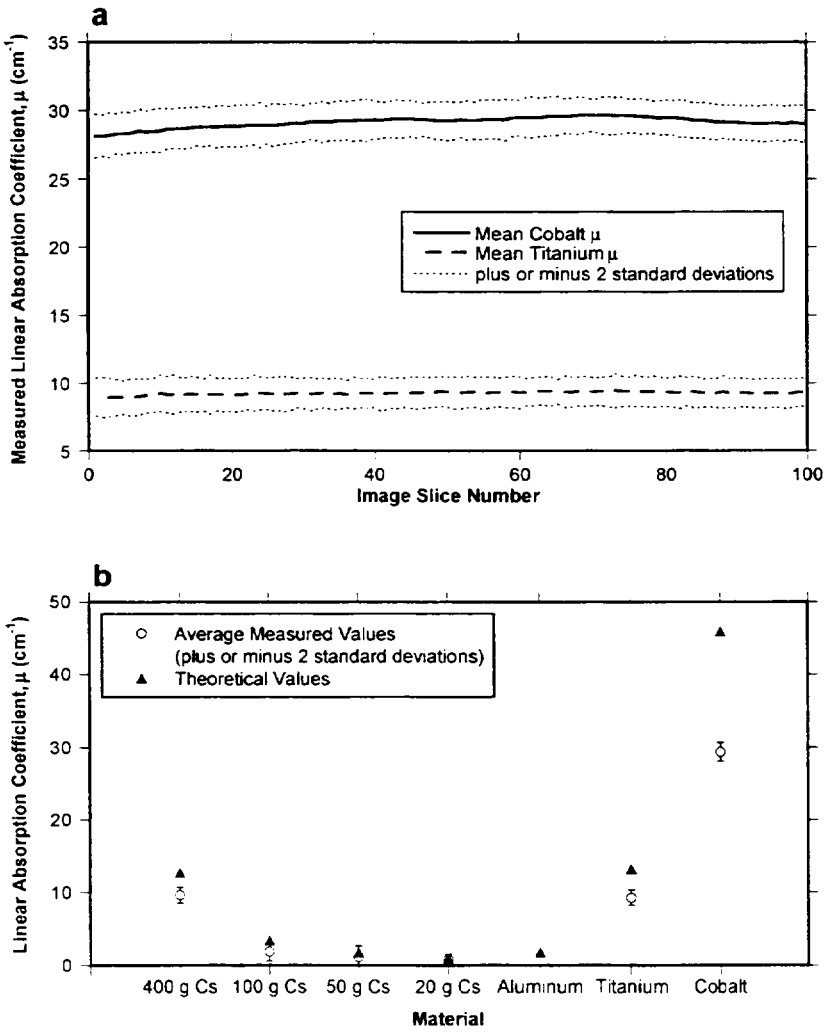

Figure 8. (a) Average and standard deviations of μ values for the region of interest for cobalt and titanium wires at 36.05 keV. (b)Measured versus theoretical linear absorption coefficient values for tubes filled with different concentrations of CsCl (given as g Cs per liter) and pure metallic wires(at 36.05 keV).

The measured linear coefficients (collected at 36.05 keV) for each of the CsCl solutions and metallic wires in comparison to the theoretical values (calculated for 36.05 keV) are shown in Figure 8b. In all cases, the theoretical values are larger than the measured values and the associated difference is larger for higher linear absorption coefficient values. The systematic nature of the discrepancy between the theoretical and measured values suggests that a relation between the two can be determined and applied as a correction to normalize the measured values. The post-processing software mentioned above would conduct this normalization as well as the noise reduction.

The observed error and noise emphasizes the importance of scanning calibration materials simultaneously with the unknown samples. Collecting images of smectite, hematite, and biotite provided calibration information on minerals with known iron content. These measurements can be compared to those of the aggregates to obtain more quantitative information on the iron content in the interstitial material in the aggregates described in Section 3.1.1.

3.3 Surface Area Measurements

Surface areas were determined to be 4.2 m^2/g for the aggregates and 5.5 m^2/g for the fine fraction. Table 2 provides a comparison of typical surface areas for a variety of soil types. The measured values fall near the low end of the distribution of observed surfaces areas for the bulk soils, and are significantly less than the values observed for the separates of clays and oxyhydroxides, such as ferrihydrite. Specific surface area for the aggregate is much higher than the surface area of spheres of comparable grain size, and is close to values reported for young alluvial soils (White, et al., 1996). These surface area values provide further evidence for the porous nature of the interstitial material. It is interesting to note that the aggregate sample exhibits a surface area that is not significantly lower than the value obtained for the fine grain fraction. Although sample morphologies are quite different for the fine powder and aggregate samples (see Figure 2), the BET data and CMT images strongly indicate that the porous, intergranular surfaces of the aggregate contribute significantly to metal sorption by the soil. The clay and oxyhydroxide coatings in the intergranular regions greatly enhance the aggregate surface areas and the corresponding number of reactive and sorptive sites in the soil samples.

Table 2. BET specific surface areas of soil components for this study and as reported by others.

Material	BET Surface Area (m^2/g)	Source
Aggregate	4.2	this study
Fine-Grained	5.5	"
Bulk Soil	4.5 to 17.7	White et al. (1996)
Quartz Separates	0.1 to 0.2	"
Clay Separates	15 to 52	"
Fe oxyhydroxides	45 to 177	"
Goethite	32 to 71	Buffle (1988)
Amorphous ferric hydroxide	100 to 700	"
Kaolinite	6 to 39	Dixon and Weed (1977)

4. Summary and Conclusions

This study attained two goals: 1) demonstrating the utility of the CMT as a nondestructive technique to locate iron-bearing minerals and visualize accessible pore space and cesium sorption sites, and 2) applying these techniques to soils from the Naturita UMTRA site to provide evidence for the accessibility of cesium (as an analog for uranium) sorption sites within the soils and speculate on the mineral composition of these sorption sites.

Because of the high X-ray absorptive property of iron, it is possible to qualitatively determine the iron content of minerals. Images of the untreated aggregates clearly show that the interstitial material between the quartz and feldspar grains is both porous and iron-bearing. These interstitial materials could be clay minerals closely associated with some iron oxyhydroxide phases or iron oxyhydroxides that are porous at the sub-micron scale. In addition, discontinuous, iron-bearing coatings could be seen around the aggregates.

By differencing images taken above and below the iodine and cesium X-ray absorption edges, it was possible to visualize accessible pore space and cesium sorption sites, respectively, in soil aggregates. Images of the pore space accessible to fluid confirm the porous nature of the interstitial materials in the aggregates. However, not all of the aggregates contain this porous, iron-bearing phase. Cesium sorption sites were observed on the outside of the coatings and in the iron-rich interstitial material accessible to fluid. These sorption sites are possibly associated with the iron-bearing minerals.

This study has provided qualitative evidence of the nature of mineral surface coatings and their ability to sorb metals, such as uranium (as uranyl) onto aggregate soils at the Naturita UMTRA site in Colorado. Evidence included the demonstration of the porous nature of the aggregate grains and the accessibility of cesium sorption sites by an intergranular fluid. A method for reducing image error and background noise is suggested for further processing of CMT images. By applying this noise and error reduction method in future CMT efforts, the authors hope to more quantitatively delineate the mineral distribution (based on iron content) in the aggregate samples and specifically identify what minerals are sorbing the metals from solution.

5. References

Aagaard, P., Jahren, J. S., Harstad, A. O., Nilsen, O., and Ramm, M. (2000), "Formation of Grain-Coating Chlorite in Sandstones: Laboratory Synthesised vs. Natural Occurrences." *Clay Minerals* 35, 261-269.

Barrett, E.P., Joyner, L.G., and Halenda, P.H. (1951), "The Determination of Pore Volume and Area Distributions in Porous Substances." *Journal of American Chemical Society,* 73, 373-380.

Buffle, J. D. (1988) *Complexation Reactions in Aquatic Systems: An Analytical Approach* Ellis Horwood, Chichester.

Coker, D. A. and Torquato, S. (1995). "Extraction of Morphological Quantities from a Digitized Medium." *Journal of Applied Physics*, 77, 6087-6099.

Criscenti, L. J., Eliassi, M., Cygan, R. T., Jové Colón, C. (2002) *Effects of Adsorption Constant Uncertainty on Contaminant Plume Migration: One- and Two-Dimensional Numerical Studies.* U.S. Nuclear Regulatory Commission NUREG/CR6780.

Curtis, G. P., Davis, J. A., Kohler, M., and Meece, D. M. (2001). "Reactive Transport Modeling of U(VI) in Groundwater at a Former Mill Site." *12th V. M. Goldschmidt Conference*, Hot Springs, VA, May 2001.

Davis, J. A., Curtis, G. P., and Naftz, D. L. (1999). "Characterization of the Naturita, Colorado Field Site and Field Sampling." *U.S. Geological Survey Letter Report to the Nuclear Regulatory Commission*, November 30, 1999.

Denison, C., Carlson, W. D., and Ketcham, R. A. (1997). "Three-Dimensional Quantitative Textural Analysis of Metamorphic Rocks using High-Resolution Computed X-Ray Tomography: Part I: Methods and Techniques." *Journal of Metamorphic Geology*, 15, 29-44.

Dixon, J.B., and Weed, S. B. (1977). *Minerals in Soil Environments.* Soil Science Society of America Book Series, Soil Science Society of America, Madison, WI.

Ehrenberg, S. N. (1993). "Preservation of Anomalously High Porosity in Deeply Buried Sandstones by Grain-Coating Chlorite: Examples from the Norwegian Continental Shelf." *American Association of Petroleum Geologists Bulletin*, 77, 1260-1286.

Flannery, B. P., Deckman, H. W., Roberge, W. G., and D'Amico, K. L. (1987). "Three-Dimensional X-Ray Microtomography." *Science*, 237, 1439.

Herman, G. T. (1980) *Image Reconstruction from Projections: The Fundamentals of Computerized Tomography.* New York: Academic Press, 316 pp.

Jenne, E. A. (1998) *Adsorption of Metals by Geomedia*, Academic Press, San Diego, 583 pp.

Jové Colón, C. F., Sanpawanitchakit, C. Xu, H. Cygan, R. T., Davis J. A., and Meece, D. M. (2002). *A Combined Analytical Study to Characterize Uranium Soil Contamination: The Case of the Naturita UMTRA Site and the Role of Grain Coatings in Composite Soil Material.* U.S. Nuclear Regulatory Commission NUREG/CR *in press.*

Kohler, M., Meece, D. M., and Davis, J. A. (2001). "A Comparison of Methods for Estimating Sorbed Uranium(VI) in Contaminated Sediments." *12th V. M. Goldschmidt Conference*, Hot Springs, VA, May 2001.

Krumhansl, J.L., Brady, P.V., and Anderson, H.L. (2001). "Reactive Barriers for ^{137}Cs Retention." *Journal of Contaminant Hydrology*, 47. 233-240.

Lide, D. R., (1991) *Handbook of Chemistry and Physics*, 71st Edition, CRC Press Inc.

Macedo, A., Vaz, C. M. P., Naime, J. M., Cruvinal, P. E., and Crestana, S. (1999). "X-Ray Microtomography to Characterize the Physical Properties of Soil and Particulate Systems." *Powder Technology*, 101, 178-182.

McMaster, W. H., Kerr Del Grande, N., Mallett, J. H., and Hubbell, J. H. (1969) "Compilation of X-Ray Cross Sections." *Lawrence Livermore National Laboratory Report*, UCRL-50174 Section II Revision I.

Rivers, M.L., Sutton, S.R., and Eng, P. (1999). "Geoscience Applications of X-Ray Computed Microtomography," *Proceedings of SPIE, Developments in X-Ray Tomography II*, Vol 3772, 78-86.

Schwartz, L. M., Auzerais, F., Dunsmuir, J., Martys, N., Bentz, D. P. and Torquato, S. (1994). "Transport and Diffusion in Three-Dimensional Composite Media." *Physica A*, 207, 28-36.

Spanne, P., Thovert, J. F., Jacquin, C. J., Lindquist, W. B., Jones, K. W., and Adler, P. M. (1994). "Synchrotron Computed Microtomography of Porous Media: Topology and Transports." *Physical Review Letters*, 73, 2001-2004.

Teter, D. M. and Cygan, R. T. (2002) *Large-Scale Molecular Dynamics Simulations of Metal Sorption onto the Basal Surfaces of Clay Minerals.* U.S. Nuclear Regulatory Commission NUREG/CR-6757, 8-2.

White, A. F., Blum, A. E., Schulz, M. S., Bullen, T. D., Harden, J. W., and Peterson, M. L. (1996). "Chemical Weathering of a Soil Chronosequence on Granitic Alluvium. I. Quantification of Mineralogic and Surface Area Changes and Calculation of Primary Silicate Reaction Rates." *Geochimica. Cosmochimica. Acta.* 60. 2533-2550.

NRC FORM 335 (2-89) NRCM 1102, 3201, 3202

U.S. NUCLEAR REGULATORY COMMISSION

BIBLIOGRAPHIC DATA SHEET

(See instructions on the reverse)

1. REPORT NUMBER (Assigned by NRC, Add Vol., Supp., Rev., and Addendum Numbers, if any.)

NUREG/CR-6784

2. TITLE AND SUBTITLE

Use of Computerized Microtomography to Examine the Relationships of Sorption Sites in Alluvial Soils to Iron and Pore Space Distributions

3. DATE REPORT PUBLISHED

MONTH	YEAR
July	2002

4. FIN OR GRANT NUMBER

W6811

5. AUTHOR(S)

McLain, Angela, A., Susan J. Altman, Mark L. Rivers, and Randall T. Cygan

6. TYPE OF REPORT

Technical

7. PERIOD COVERED *(Inclusive Dates)*

December 1999 to April 2002

8. PERFORMING ORGANIZATION - NAME AND ADDRESS *(If NRC, provide Division, Office or Region, U.S. Nuclear Regulatory Commission, and mailing address; if contractor, provide name and mailing address.)*

Geochemistry Section
Sandia National Laboratories
Albuquerque, NM 87185 - 0750

9. SPONSORING ORGANIZATION - NAME AND ADDRESS *(If NRC, type "Same as above"; if contractor, provide NRC Division, Office or Region, U.S. Nuclear Regulatory Commission, and mailing address.)*

Division of Systems Analysis and Regulatory Effectiveness
Office of Nuclear Regulatory Research
U.S. Nuclear Regulatory Commission
Washington, DC 20555-0001

10. SUPPLEMENTARY NOTES

Edward O'Donnell, NRC Project Manager

11. ABSTRACT *(200 words or less)*

This report represents results from computerized microtomographic (CMT) imaging of soils from Naturita, Colorado, a Uranium Mill Tailings Remedial Action (UMTRA) site. The objective is to better understand the mineralogical and morphological controls of the sorption of uranium in the sediments. The samples were prepared and imaged with three goals in mind: (1) to visualize iron-rich mineral distribution in fine-grained materials (<355 microns grain size) and aggregate grains, (2) to visualize pore space in the aggregates, and (3) to visualize cesium sorption sites as a proxy for uranium. Two sets of images were obtained with the voxel sizes of 6.7 microns and 3.3 microns on a side, respectively. Bright rims with a thickness of 4 to 15 microns were observed on fine-grained materials and aggregate grains. Porous, iron-rich interstitial material was also observed within the aggregates. It is speculated that these interstitial materials are clay minerals closely associated with some iron oxyhydroxide phases or iron oxyhydroxides that are porous at the sub-micron scale. However, to verify this identification, the CMT data needs to be post-processed using calibration materials to minimize noise and error. A subtraction technique using images obtained just above and below the X-ray absorption edges of iodine and cesium successfully illustrates the pore space distribution in the KI saturated samples and sorption sites in CsCl- treated samples. The cesium sorption sites appear to be associated with accessible pore space observed in the untreated and KI saturated samples. The cesium sorption sites are also associated with iron-rich areas both as exterior coatings and in the interstitial areas of the aggregate grains.

12. KEY WORDS/DESCRIPTORS *(List words or phrases that will assist researchers in locating the report.)*

microtomography, sorption, sorption mechanisms, uranium sorption,

13. AVAILABILITY STATEMENT

unlimited

14. SECURITY CLASSIFICATION

(This Page) unclassified

(This Report) unclassified

15. NUMBER OF PAGES

16. PRICE

Federal Recycling Program